DOI: 10.1002/ejoc.200600437

Long Chain-Substituted and Triply Functionalized Molecular Knots – Synthesis, Topological Chirality and Monolayer Formation

Athanasia Böhmer,[a] Jens Brüggemann,[a] Astrid Kaufmann,[a] Albena Yoneva,[a] Sonja Müller,[a] Walter M. Müller,[a] Ute Müller,[a] Frank W. Vergeer,[b] Lifeng Chi,[b] Luisa De Cola,[b] Harald Fuchs,[b] Xiaoming Chen,[c] Takateru Kubota,[d] Yoshio Okamoto,[d] and Fritz Vögtle*[a]

Keywords: Supramolecular chemistry / Template synthesis / Molecular knots / Topological chirality / Enantiomer separation

New topological chiral molecular knots (knotanes) **3a**–**6** of the amide type were substituted with long aliphatic side chains (butyloxy, hexyloxy, octenyloxy, decyloxy) and with *p*-bromobenzyloxy and oligoethylene glycol ether units, which resulted in improved solubility and enhanced potential for racemate separation. In consequence, the knotanes with longer substituted chains could be separated even on commercially available noncovalently bound chiral stationary phases. The (*p*-bromobenzyloxy)-knotane **6** and the octenyloxy-knotane **4** were synthesized with the intention of using their functional sidechains in further reactions, **6** being used in Suzuki-type reactions, while **4** was consequently allowed to react in the presence of Grubbs catalyst in metathesis reactions. The achieved solubility allowed us to test the abilities of the alkyl chain-substituted knotanes **3a**–**c** and the (*p*-bromobenzyloxy)-knotane **6** to form Langmuir–Blodgett films. The assemblies were investigated on mica by AFM technique. A key point of focus was the (topological) chirality of the long chain-substituted knotanes. To address this point, the racemates were enantioseparated by HPLC on various chiral phases, and the obtained pure enantiomers were found to exhibit pronounced Cotton effects in their circular dichroism spectra. The absolute configurations of all new knots were derived by comparison with the unsubstituted knot.

1. Concept and Synthesis

Since 2000 we have produced over a dozen grams of molecular knots[1–3] of the amide type.[4–7] Whilst the presence of any substituent in the 5-position of the isophthalic unit reduces the yield of the knot or even prevents its formation, substitution in the 4-position of the pyridine unit is possible, even with larger substituents, without reduction of the yield of the knotane.[5] As previous X-ray crystal structure analyses of corresponding knotanes[4,6a] have shown, this can be explained by the location of the pyridine units at the periphery of the knot, whilst the isophthalic units are buried inside the knot structure.

[a] Kekulé-Institut für Organische Chemie und Biochemie der Rheinischen Friedrich-Wilhelms-Universität Bonn,
Gerhard-Domagk-Str. 1, 53121 Bonn, Germany,
Fax: +49-228-735662
E-mail: voegtle@uni-bonn.de
[b] Physikalisches Institut, Westfälische Wilhelms-Universität Münster,
Wilhelm-Klemm-Str. 10, 48149 Münster, Germany
[c] EcoTopia Science Institute, Nagoya University,
Furo-cho, Chikusa-ku, Nagoya, 464-8603 Japan
[d] Department of Applied Chemistry, Graduate School of Engineering, Nagoya University,
Chikusa-ku, Nagoya, 464-8603 Japan

We have therefore investigated substitution with aliphatic chains on the pyridine rings. The production of long chain-substituted knots opens the following interesting possibilities:

a) The long aliphatic chains, and especially the oligoethylene glycol ether chains, were expected to increase the solubility strongly, which would be valuable not only for subsequent chemical reactions, but also for chromatographic separations, HPLC enantiomer separations in particular. In the latter case we have thus far had to use highly lipophilic solvents to dissolve the chiral unsubstituted knots, and these cause commercial chiral phases, especially noncovalently bound ones, to bleed out.

b) The fixation of one or more long chains at one knot molecule would allow the introduction of the highly "nanochiral" knot unit into lipophilic membranes, establishing high optical activity.

c) The presence of functional chains would allow for further functionalization of a knotane at its periphery. The *p*-bromobenzyloxy groups in knotane **6** could be refunctionalized through C–C coupling reactions (e.g., the Suzuki-coupling reaction), whereas the octenyloxy group in **4** would offer the potential for, for example, olefin metathesis (once, twice or three times) or the coupling of the three peripheral

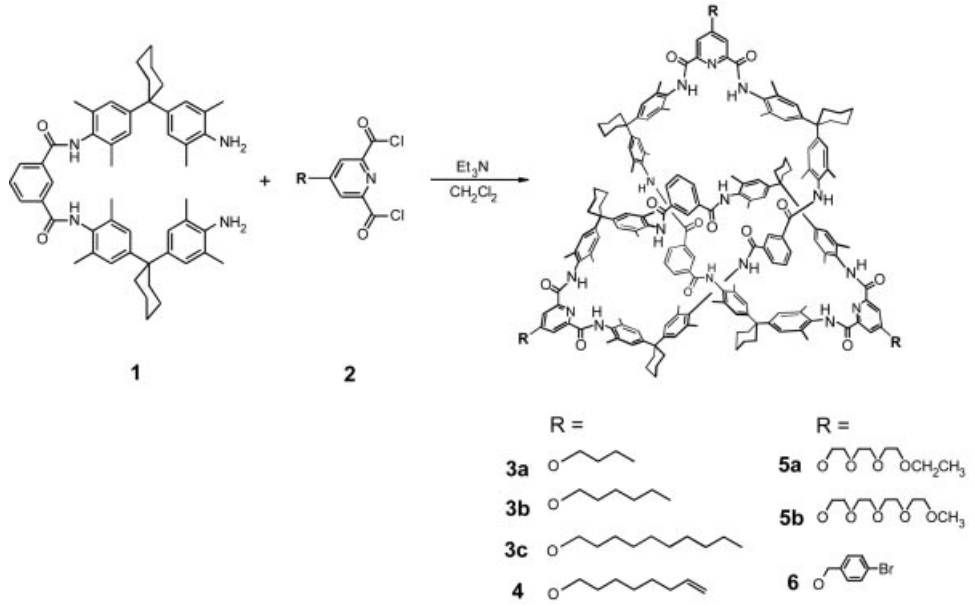

Figure 1. Synthesis of long chain-substituted knots **3a**–**6**.

double bonds in the presence of Grubbs catalyst to yield a triply bridged double knot.

For the synthesis of long chain-substituted molecular knots we started from the "extended" diamine **1**[4] and the substituted pyridinedicarboxylic acid dichloride **2** (Figure 1). The one-pot syntheses were carried out under moderate dilution conditions (approx. 1.5 mM) in dichloromethane. Under these conditions the reactions yielded 3% of pure knot **3b**, 5% of **4** and **6** and 4% of **3a** and **3c**, after triple purification by column chromatography over silica gel. The oligoethylene glycol ether-substituted knotanes **5a** and **5b** were identified by MALDI-TOF spectroscopy but could not easily be isolated in pure form because of the presence of coexisting monomacrocyclic byproducts with very similar R_f values. Separation of **5a** and **5b** from the cyclic octalactam byproducts and the enantiomer separations of the knotanes could, however, be performed by HPLC.

2. Enantiomer Separation and Circular Dichroism

The introduction of long chains into the knotane structure indeed proved advantageous, resulting in the anticipated improvements in solubility that expand the possibilities for chiral separation. Because of their limited solubilities the enantiomer separation of the knots with smaller chains, such as butyloxy (**3a**) and hexyloxy (**3b**), was only successful when immobilized "Chiralpak®AD" column material[8] was used (see Figure 2, parts a and b). This only recently commercially available column material contains tris-(3,5-dimethylphenylcarbamate)amylose covalently bound to the silica gel support, thereby making it impossible for the chiral stationary phase (CSP) to be washed out, even if lipophilic solvents are used. Use of an *n*-hexane/chloroform/propan-2-ol mixture (300:200:1) as eluent and a flow rate of 0.5 mL min^{-1} showed separation factors α = 1.56 for the chiral separation of **3a** and α = 1.62 for **3b**. Unlike **3a** and **3b**, the knots with longer chains, such as octenyloxy **4** and decyloxy **3c**, show enhanced solubilities, which allowed us to carry out their complete enantiomer separation, with commercially available columns. The resolution of **4** could consequently be carried out on a commercial Nucleosil®-Chiral-2 column with an *n*-hexane/propan-2-ol mixture (70:30) as a mobile phase and a flow rate of 1 mL min^{-1}, giving a separation factor of α = 1.26 (Figure 2, d). An *n*-hexane/ethanol mixture (88:12) as a mobile phase and a flow rate of 0.8 mL min^{-1} showed a separation factor α = 1.245 for the enantiomeric resolution of **3c** on a commercial noncovalent Chiralcel®OD material[9] (Figure 2, c), whilst the enantiomer separation of the (*p*-bromobenzyloxy)-knotane **6** was successful on a commercial Nucleosil®-Chiral-2 column with *n*-hexane/propan-2-ol (50:50) as eluent and a flow rate of 0.7 mL min^{-1} (Figure 2, e). The resolution of **5b** could be achieved on a Chiralpak®IB[10] column with *n*-hexane/dichloromethane/propan-2-ol (70:20:10) as eluent and a flow rate of 1.0 mL min^{-1} (Figure 2, f).[11]

After the preparative separation of the enantiomers, circular dichroism spectra were recorded. The pure enantiomers exhibit pronounced Cotton effects in their circular dichroism spectra. By comparison with the enantiomers of the unsubstituted knot[4,6a] it was possible to derive the absolute configurations of all new knots, as the analogy of the Cotton effects is pronounced. In consequence we have assigned the Λ configuration to the (+) enantiomers. Figure 3 shows the CD spectra of **3a** and **6** as representative examples, whilst the absolute configurations of the two enantiomers of a trefoil knot with Δ and Λ stereochemistry are shown schematically in Figure 4.

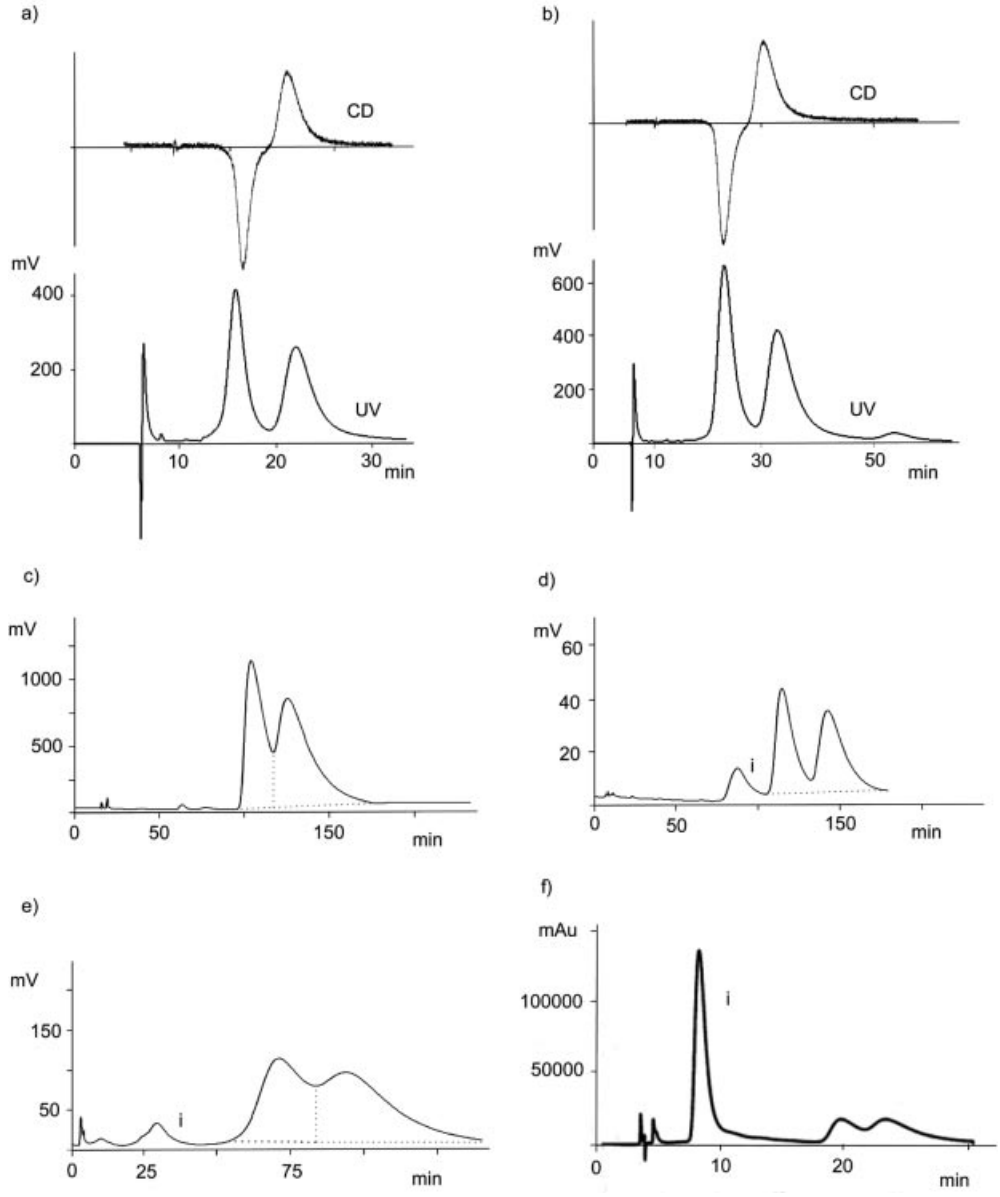

Figure 2. Separation of the enantiomers of: a) and b) **3a** and **3b** (column: Chiralpak®AD, eluent: *n*-hexane/chloroform/propan-2-ol (300:200:1), CD detection at 254 nm), c) **3c** [column: Chiralcel®OD, eluent *n*-hexane/ethanol (88:12)], d) **4** (column: Nucleosil®-Chiral-2, eluent: *n*-hexane/propan-2-ol (70:30), i = cyclic octalactam (byproduct), e) **6** (column: Nucleosil®-Chiral-2, eluent: *n*-hexane/propan-2-ol (50:50), i = cyclic octalactam (byproduct), and f) **5b** [column: Chiralpak IB, eluent: *n*-hexane/dichloromethane/propan-2-ol (70:20:10), i = cyclic octalactam (byproduct)].

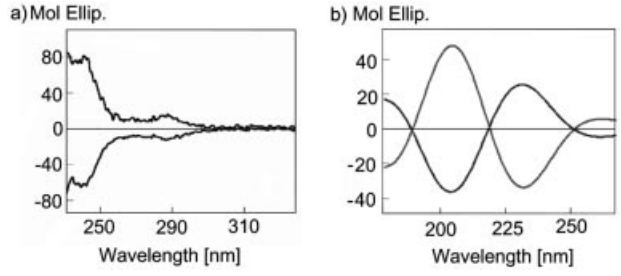

Figure 3. Circular dichroism spectra of: a) **3a** [d = 0.1 mm, chloroform, (+) enantiomer $c = 4.95 \cdot 10^{-4}$ M, (–)-enantiomer $c = 8.92 \cdot 10^{-4}$ M], and b) **6** [d = 0.1 mm, trifluoroethanol, (+)-enantiomer $c = 2.9 \cdot 10^{-4}$ M, (–)-enantiomer $c = 1.1 \cdot 10^{-4}$ M].

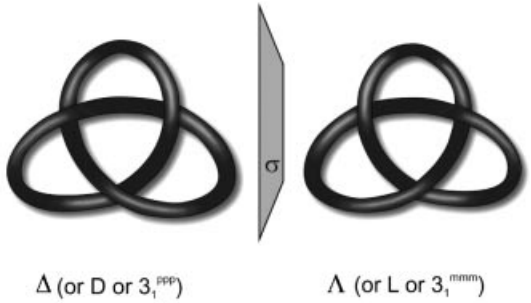

Figure 4. Configurations of the enantiomers of the trefoil knot.[2c]

3. Langmuir–Blodgett Films

The film-forming properties[12] of the alkyl chain-substituted knotanes were studied by spreading aliquots of dichloromethane solutions of the compounds on pure water (Millipore, 18.2 MΩ) at 21 °C. Typical surface pressure/molecular area (π/A) isotherms were recorded for the knotanes **3a**–**c** and **6**, as shown in Figure 5. The average limiting areas per molecule, obtained by extrapolating the condensed phase region of the isotherm to zero pressure, are summarized in Table 1.

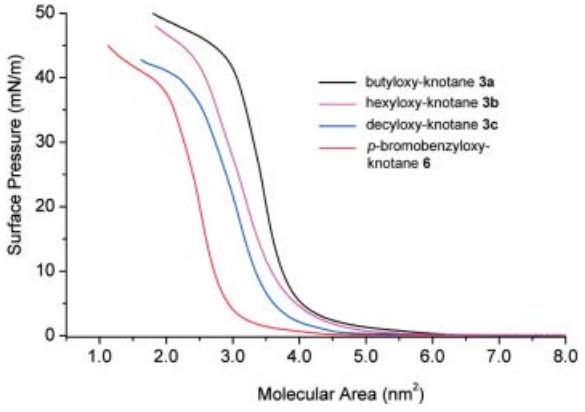

Figure 5. π/A Isotherms of Langmuir films of various molecular knots (conditions are given in the text).

Table 1. Average limiting areas per molecule obtained from the π/A isotherms.

Knotane	Average limiting area per molecule (nm^2)
Decyloxy-knotane **3c**	3.9
Hexyloxy-knotane **3b**	3.6
Butyloxy-knotane **3a**	2.9
(*p*-Bromobenzyloxy)-knotane **6**	3.8

In all cases the isotherms display steep pressure increases, which correspond with the formation of condensed phases. The average limiting areas per molecule range from 3.9 to 2.9 nm^2 and decrease in the order decyloxy-, *p*-bromobenzyloxy, hexyloxy- and butyloxy-knotane. The reduction in the molecular area with decreasing length of the alkyl chain is too large to be directly related to the number of carbons in the chain that have been removed. With regard to the positions of the chains in the different molecules, the 3D structures of the molecules need to be considered in order to make firm statements about the molecular orientations and the structures of the Langmuir films. From the thicknesses of the obtained LB films (ca. 1.6 nm, vide infra), however, it seems that the molecules form Langmuir monolayers.

Hysteresis experiments were performed in order to study the reversibility of the Langmuir film formation, as shown in Figure 6. The results obtained for the decyloxy-knotane **3c** in these compression-expansion experiments were slightly different than those for the other three molecules: upon expansion of a previously compressed film, the surface pressure does not completely go back to zero, indicating that certain aggregates persist. A very small shift of the isotherm to a smaller molecular area is observed upon recompression, which points either to the loss of molecules to the subphase or to the occurrence of reorganization processes resulting in non-monomolecular structures. After the second expansion cycle, however, the molecular area remains constant. In the other three knotane samples significantly more hysteresis was revealed in the isotherms, with larger shifts to smaller mean molecular areas being observed (see the inset of Figure 6 for butyloxy-knotane **3a**). The observed hystereses, together with the shifts of the isotherms to smaller average limiting areas, indicate that the Langmuir film formation is not completely reversible and that the obtained films are not completely stable under the employed nonequilibrium conditions.

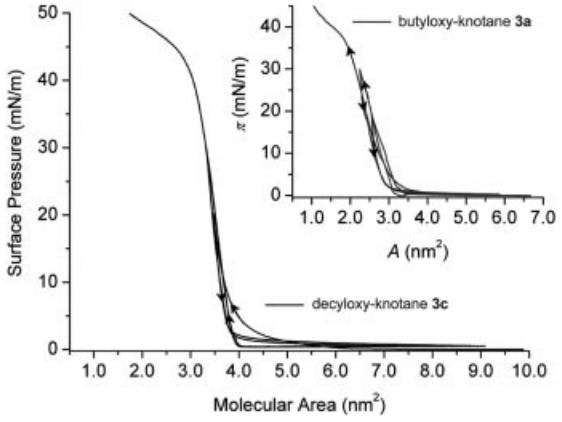

Figure 6. Compression/expansion isotherms for the knots **3a** and **3c**.

Langmuir films of the different knotane molecules were transferred onto freshly cleaved mica substrates by the vertical dipping method (upstroke) and studied by scanning force microscopy. The films were transferred at surface pressures of 30 and 40 $mN\,m^{-1}$ (40 and 45 $mN\,m^{-1}$ for decyloxy-knotane **3c**). Although the fluctuations in the transfer surface pressure were smaller at a transfer pressure of 40 $mN\,m^{-1}$, the obtained AFM images show rather homogeneous films (Figure 7, a) for all knotanes at both 30 and 40 $mN\,m^{-1}$. In general, it was quite difficult to acquire well resolved AFM images as the films were very smooth and soft. In the case of the (*p*-bromobenzyloxy)-knotane **6** the film showed defects (Figure 7, b) large enough to allow a reliable height measurement, and the film thickness was measured as 1.6 nm, which is consistent with the molecular dimensions. From the thickness obtained from AFM it is reasonable to conclude that we had obtained monomolecular layers of knotane molecules here.

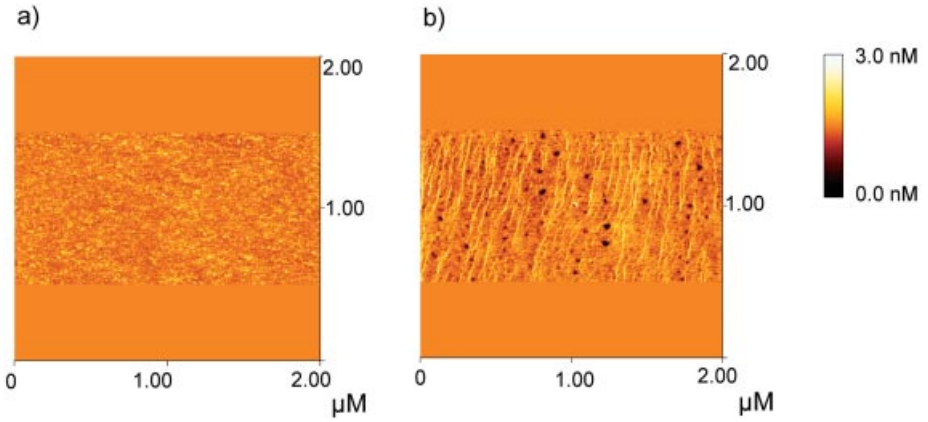

Figure 7. AFM images (2 μm × 2 μm) of Langmuir–Blodgett films (on mica) of a) hexyloxy-knotane **3b** and b) (*p*-bromobenzyloxy)-knotane **6**, transferred at 40 mN m^{-1}.

4. Chemical Reactions with Functionalized Knotanes

a. Reactions with the Octenyloxy-knotane 4

The octenyloxy-substituted knotane **4** was treated with styrene under olefin metathesis conditions,[13] yielding singly, doubly and triply styrene-substituted knotanes **7a**–**c** (Figure 8), which were identified by MALDI-TOF spectroscopy but have not yet been isolated in pure form due to the similar chromatographic behaviour of the octenyloxy- and styrene-substituted knots.

The metathesis reaction can also be used to create a new oligo-knot architecture by coupling the long chain-substituted knot **4** with itself, providing a triply bridged double knot **8** (see Figure 9). Orientational results (MALDI-TOF) show that **8** is indeed formed, although in low yield. Its attempted isolation by HPLC chromatography proved difficult, due to the formation of oligomeric byproducts.

b. Reactions of the (*p*-Bromobenzyloxy)-knotane 6

The reaction behaviour of the cyclic dimer **9**, as a model compound, shows that the introduction of a pyrene unit can be achieved through a Suzuki coupling reaction[14] with 4,4,5,5-tetramethyl-2-(pyren-1-yl)-1,3,2-dioxaborolane (**10**) in the presence of 2′-dicyclohexylphosphanyl-2′,6′-dimethoxy-biphenyl (**L***, Figure 10).

After the successful coupling of model compounds **9** and **10** to yield **11**, the (*p*-bromobenzyloxy)-knotane **6** was coupled in an analogous Suzuki reaction, yielding a pyrene-substituted knotane **12** (see Figure 11), bearing three pyrene units, as indicated by MALDI-TOF measurements.

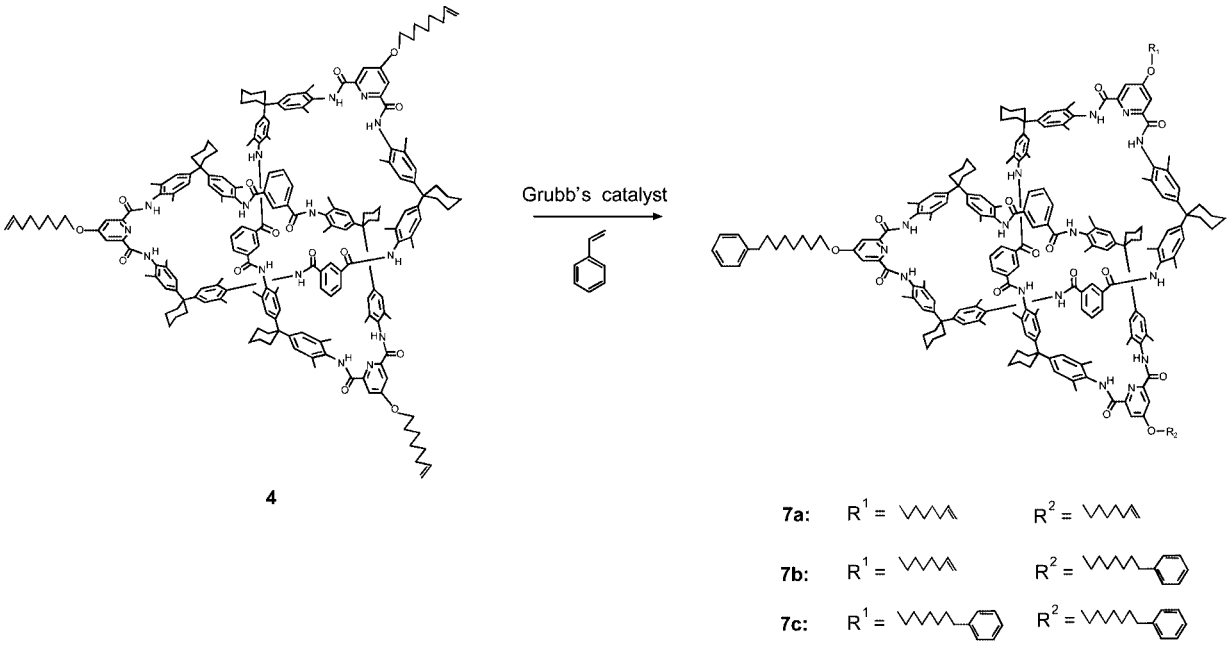

Figure 8. Synthesis of styrene-substituted knotanes **7a**–**c**.

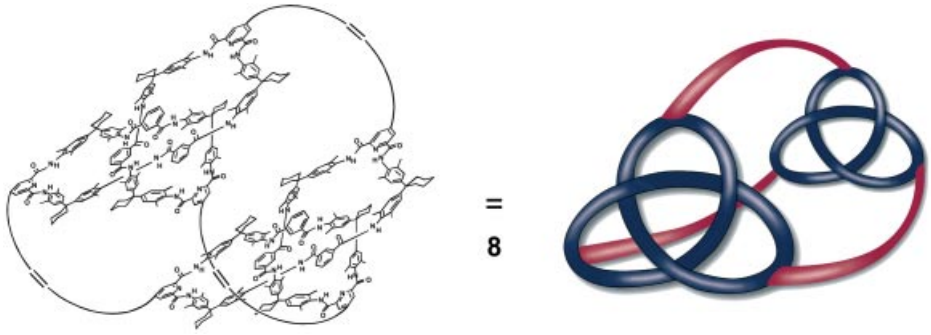

Figure 9. Schematic structure of double knot **8**.

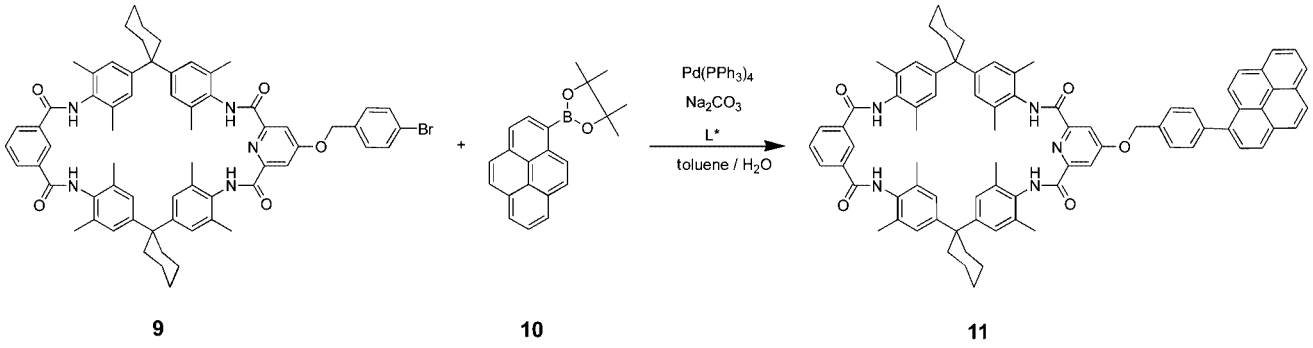

Figure 10. Synthesis of model complex **11** through a Suzuki coupling reaction.

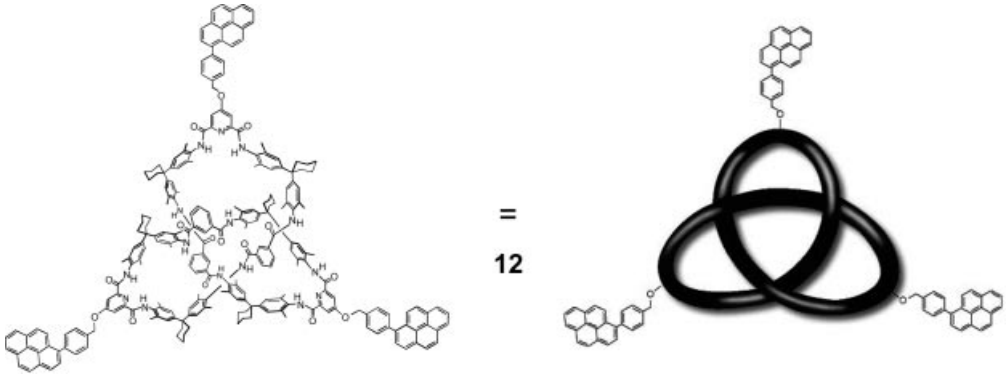

Figure 11. Schematic structure of the pyrene-substituted knotane **12**.

5. Conclusions

For the first time we have synthesized pure, readily soluble and completely enantiomerically separable, topologically chiral molecular knots with long-chain substituents. The compounds show enhanced solubilities, allowing the easy separation of their racemic mixtures into the pure enantiomers by HPLC.

The functionalized knotanes were shown to form fairly homogeneous Langmuir–Blodgett films, with the exception of knotane **6**, for which a distinct number of defects were observed. AFM measurements on film thicknesses indicate that knotane molecules form monomolecular layers by LB preparation.

The new functionalized knotanes can be further functionalized at their peripheries, by using distant haloaryl groups or double bonds as reactive groups in Suzuki-type C–C coupling or metathesis reactions, yielding new knot derivatives and new oligo-knot architectures. In addition, the new knotane structures may prove to be valuable candidates for the implantation of knot structures with high chirality in membranes.

Experimental Section

General Remarks: All starting materials were purchased from commercial sources or prepared by known literature procedures. The

solvents were dried by standard techniques. Whenever possible, reactions were monitored by thin-layer chromatography on TLC silica gel $60F_{254}$ (Merck) aluminium plates. Compounds were detected with UV light (254 nm). Melting points were determined with a Reichert Thermovar microscope and are uncorrected. ^1H and ^{13}C NMR spectra were recorded with 400 and 500 MHz Bruker instruments; the solvent signals were used for internal calibration. Mass spectra were recorded with a Concept 1H instrument from Kratos Analytical Ltd., Manchester, a MALDI-TofSpec-E machine from MICROMASS, GB (MALDI) and a Voyager-DE from PE Biosystems (MALDI). The enantiomer separations were achieved on Chiralpak AD columns (250 × 4 mm, for **3a** and **3b**), a Chiralcel OD column (250 × 10 mm, 20 μm, for **3c**), a Chiralpak IB column (250 × 4.6 mm, for **5b**) and Nucleosil 100-5 Chiral-2 columns (250 × 4 mm, for **4** and **6**).

Langmuir–Blodgett Films and AFM Investigations: Surface pressure/molecular area (π/A) isotherms were measured with the aid of a thermostatted Langmuir trough fitted with a commercial Wilhelmy balance (KSV 3000, Finland). The trough was filled with pure deionized water (Millipore, resistance 18 MΩ cm). The knotane samples were dissolved in CH_2Cl_2 (HPLC, Fluka) to provide 1.2–1.3 × 10^{-4} M spreading solutions. Langmuir monolayers were prepared at 20 ± 1 °C by carefully spreading the stock solution (100–150 μL) on the cleaned surface of the subphase and compressing the floating molecules at a barrier speed of 5 mm min^{-1}. Langmuir–Blodgett films were deposited from the air/water interface onto freshly cleaved mica surfaces (Plano, Germany) by the vertical dipping method at a transfer rate of 1 mm min^{-1} and at surface pressures of 30, 40 and 45 mN m^{-1}. AFM investigations were performed with a commercial Nanoscope IIIa, Dimension 3000 microscope (Digital Instruments, Santa Barbara, CA), operating in tapping mode under ambient conditions and with use of silicon cantilevers (Nanoworld) with spring constants of 296–350 kHz.

General Procedure for the Synthesis of Knotanes 3a–6: A solution of the substituted pyridine-2,6-dicarbonyl chloride **2** (1.55 mmol; for knotane **6**: 1.79 mmol) in dry dichloromethane (250 mL) and a solution of *N*,*N*′-bis{4-[1-(4-amino-3,5-dimethylphenyl)cyclohexyl]-2,6-dimethylphenyl}isophthalamide (**1**) (1.2 g, 1.55 mmol; for knotane **6**: 1.39 g, 1.79 mmol) in dry dichloromethane (250 mL) with triethylamine (0.7 mL) were simultaneously introduced into a stirred flask containing dry dichloromethane (700 mL) over a 7 h period. After the addition was complete, the reaction mixture was stirred overnight. The solvent was removed under reduced pressure and the products were purified by three consecutive chromatographic runs over silica gel, with use of dichloromethane/acetone (20:1), dichloromethane/acetone (10:1) and dichloromethane/ethyl acetate (4:1) as eluents.

Knotane 3a: This compound was obtained from 4-butyloxy-2,6-pyridinedicarbonyl chloride (0.48 g); yield: 60 mg (4%).

Knotane 3b: This compound was obtained from 4-hexyloxy-2,6-pyridinedicarbonyl chloride (0.47 g); yield: 47 mg (3%).

Knotane 3c: This compound was obtained from 4-decyloxy-2,6-pyridinedicarbonyl chloride (0.56 g); yield: 65 mg (4%).

Knotane 4: This compound was obtained from 4-(7-octen-1-yloxy)-2,6-pyridinedicarbonyl chloride (0.51 g); yield: 78 mg (5%).

Knotane 5a: This compound was obtained from 4-(2-{2-[2-(2-methoxyethoxy)ethoxy]ethoxy}ethoxy)-2,6-pyridinedicarbonyl chloride (0.66 g).

Knotane 5b: This compound was obtained from 4-{2-[2-(2-ethoxy)-ethoxy]ethoxy}-2,6-pyridinedicarbonyl chloride (0.61 g).

Knotane 6: This compound was obtained from 4-(4-bromobenzyloxy)-2,6-pyridinedicarbonyl chloride (0.7 g); yield: 60 mg (5%).

Only well resolved signals in the ^1H NMR spectra are referenced below.

Butyloxy-knotane 3a: M.p. > 250 °C; ^1H NMR (400 MHz, [D_6]-DMSO): δ = {0.01, 0.79, 0.89, 1.13, 1.18, 1.31, 1.41, 1.43, 1.51, 1.74 (br.), 1.93, 2.10, 2.13, 2.19, 2.22, 2.26, 2.44 (m), 3.24} (153 H, CH_2 *c*Hex and butyl, CH_3 butyl and $ArCH_3$), 4.21 (br., 6 H, OCH_2), {4.94, 5.78, 6.57, 7.48} (m, 4 H, isoH) {5.24, 6.39, 6.47, 6.75, 6.90, 6.93, 6.98, 7.11, 7.38, 7.50, 7.61, 7.71, 7.72, 7.77, 7.78, 7.84, 7.86 (br.)} (36 H, ArH), {8.22, 8.52, 8.99, 9.07, 9.31, 9.51, 9.74, 10.16, 10.42, 10.46, 10.93, 10.94} (12 H, NH) ppm. MALDI-TOF: *m*/*z*: calcd. for $C_{189}H_{213}N_{15}O_{15}$: 2934.8; found: 2934.1 $[M]^+$, 2955.6 $[M + Na]^+$.

Hexyloxy-knotane 3b: M.p. > 250 °C; ^1H NMR (400 MHz, [D_6]-DMSO): δ = {0.02, 0.83 (br.), 0.90, 1.08, 1.18, 1.26 (br.), 1.30, 1.40 (br.), 1.49, 1.71 (br.), 1.92, 2.06, 2.13 (br.), 2.19, 2.22, 2.26, 2.43, 2.44 (m)} (165 H, CH_2 *c*Hex and hexyl, CH_3 hexyl and $ArCH_3$), 4.20 (br., 6 H, OCH_2), {4.93, 5.73, 6.59, 7.46} (m, 4 H, isoH) {4.46, 5.28, 6.35, 6.39, 6.46, 6.75 (br.), 6.85 (br.), 6.90, 6.93, 7.10 (br.), 7.29 (br.), 7.38, 7.50, 7.52, 7.67, 7.70, 7.72, 7.76, 7.78, 7.84 (br.)} (36 H, ArH), {8.22, 8.52, 8.99, 9.07, 9.31, 9.51, 9.74, 10.15, 10.42, 10.46, 10.93, 10.94} (12 H, NH) ppm. MALDI-TOF: *m*/*z*: calcd. for $C_{195}H_{225}N_{15}O_{15}$: 3018.9; found: 3018.8 $[M]^+$, 3039.6 $[M + Na]^+$, 3056.5 $[M + K]^+$.

Decyloxy-knotane 3c: M.p. > 250 °C; ^1H NMR (400 MHz, [D_6]-DMSO): δ = {0.02, 0.81(br.), 0.90, 0.94, 1.20 (br.), 1.31, 1.43 (br.), 1.52, 1.75 (br.), 1.94, 2.06, 2.16 (br.), 2.23, 2.25, 2.30, 2.46 (m), 3.35 } (189 H, CH_2 *c*Hex and decyl, CH_3 decyl and $ArCH_3$), 4.18 (br., 6 H, OCH_2), {4.94, 5.81, 6.55, 7.45} (m, 4 H, isoH) {5.30, 6.31, 6.35, 6.47, 6.74 (br.), 6.84, 6.87, 6.94, 7.11 (br.), 7.27 (br.), 7.39, 7.51, 7.54, 7.67, 7.69, 7.72, 7.73, 7.78, 7.79, 7.84 (m)} (36 H, ArH), {8.27, 8.56, 8.96, 9.05, 9.26, 9.57, 9.76, 10.18, 10.45, 10.49, 10.94, 10.95} (12 H, NH) ppm. MALDI-TOF: *m*/*z*: calcd. for $C_{207}H_{249}N_{15}O_{15}$: 3187.3; found: 3186.7 $[M]^+$, 3209.7 $[M + Na]^+$, 3225.6 $[M + K]^+$.

Octenyloxy-knotane 4: M.p. > 250 °C; ^1H NMR (400 MHz, [D_6]-DMSO): δ = {0.03, 0.80 (br.), 0.90, 1.18, 1.31, 1.40 (br.), 1.52, 1.72 (br.), 1.99, 2.09, 2.11, 2.23, 2.26, 2.44 (m), 3.24 } (162 H, CH_2 *c*Hex and octenyl and $ArCH_3$), 4.21 (br., 6 H, OCH_2), 4.88–4.98 (m, 6 H, CH_2=CH) {5.28, 6.58} (m, 2 H, isoH), 5.71–5.81 (m, 3 H,CH=CH_2) {6.36, 6.40, 6.47, 6.60 (br.), 6.77 (br.), 6.85, 6.92, 6.95, 6.99 7.10 (br.), 7.30 (br.), 7.39, 7.51, 7.68, 7.69, 7.70, 7.73, 7.78, 7.79, 7.85 (m)} (38 H, ArH), {8.22, 8.54, 9.01, 9.10, 9.34, 9.57, 9.74, 10.17, 10.46, 10.54, 10.95, 10.96} (12 H, NH) ppm. MALDI-TOF: *m*/*z*: calcd. for $C_{201}H_{231}N_{15}O_{15}$: 3097.1; found: 3097.1 $[M]^+$, 3119.0 $[M + Na]^+$, 3134.7 $[M + K]^+$.

(*p*-Bromobenzyloxy)-knotane 6: M.p. >250 °C; ^1H NMR (500 MHz, [D_6]DMSO): δ = 0.80–1.60 (br., 60 H, CH_2 *c*Hex), 1.90–2.55 (br., 72 H, $ArCH_3$), 5.29 (s, 6 H, OCH_2), {5.68, 6.36, 6.38, 6.46, 6.84, 6.90, 6.93, 6.95, 6.98, 7.05, 7.46} (br., 24 H, ArH), {5.10, 6.59, 7.10} (br., 3 H, isoH), {5.79, 7.14, 7.88} (br., 3 H, isoH), {7.27, 7.51, 7.86} (br., 3 H, isoH), 7.55 (d, $^3J_{HH}$ = 8.41 Hz, 6 H, Br–ArH), 7.39 (d, $^3J_{HH}$ = 8.43 Hz, 6 H, Br–ArH), 7.74, 7.77 (br., 2 H, pyrH), 7.79 (d, 2 H, pyrH), 7.82 (d, 2 H, pyrH), {8.08, 8.22, 8.53, 8.99, 9.07, 9.32, 9.52, 9.73, 10.16, 10.45, 10.48, 10.95} (12 H, NH) ppm. MALDI-TOF: *m*/*z*: calcd. for $C_{198}H_{201}Br_3N_{15}O_{15}$: 3273.6; found: 3273.7 $[M]^+$, 3295.6 $[M + Na]^+$, 3311.9 $[M + K]^+$.

Pyrene-Substituted Tetralactam 11: Cyclic tetralactam **9** (100 mg, 0.092 mmol), 4,4,5,5-tetramethyl-2-(1-pyrenyl)-1,3,2-dioxaborolane (**10**, 37.6 mg, 0.115 mmol) and 2′-dicyclohexylphosphanyl-2′,6′-di-

methoxybiphenyl (**L***, 1.89 mg, 0.0046 mmol) were dissolved in toluene (24 mL). A solution of sodium carbonate (24.3 mg, 0.229 mmol) in water (6 mL) was added, after which the resulting mixture was flushed with argon for 15 min. After the addition of tetrakis(triphenyl)phosphanepalladium(0) (5.32 mg, 0.0046 mmol), the mixture was stirred under argon in the dark at 115 °C for 48 h. The reaction mixture was allowed to cool down to room temp. and poured into a MeOH/water mixture. The precipitate was filtered off and after leaching with dichloromethane the solvent was removed under reduced pressure and purified by column chromatography over silica gel (dichloromethane/ethyl acetate, 2:1). Yield: 48 mg (44%). ^{1}H NMR (400 MHz, $CDCl_3$): δ = 1.14 (m, 12 H, CH_2 *c*Hex), 1.43, 1.56 (m, 8 H, CH_2 *c*Hex), 2.11 (s, 12 H, $ArCH_3$), 2.14 (s, 12 H, $ArCH_3$), 5.43 (s, 2 H, O–CH_2), 6.91 (s, 8 H, ArH), 7.57 (br., 2 H, Ar-bridge), 7.62 (br., 2 H, Ar-bridge), 7.60 (m, 1 H, iso), 8.02 (m, 11 H, 9 pyrene, 2 iso), 8.90 (br., 3 H, 2 pyr, 1 iso) ppm. ^{13}C NMR (100.6 MHz, $CDCl_3$): δ = 14.21 (8 C, CH_3), 19.13 (4 C, *c*Hex), 21.00 (2 C, *c*Hex), 35.90 (4 C, *c*Hex), 37.34 (2 C, Cq), 70.81 (1 C, O–CH_2), 111.96 (2 C, pyr-$C_{3/5}$), 124.72, 124.97, 126.11, 126.64, 126.90, 127.20, 127.44, 127.57, 127.71, 127.81, 130.42, 130.99, 131.08, 131.52, 134.44, 134.63 (47 C, 20 r-C, 5 Ar bridge, 16 pyrene, 6 iso), 136.87 (1 C, Ar bridge), 141.65 (4 C, ar-Cq), 150.77 (2 C, pyr-$C_{2/6}$), 161.10 (1 C, pyr-C_4), 165.24 (2 C, C=O), 168.10, 171.24 (2 C, C=O) ppm. MALDI-TOF: *m*/*z*: calcd. for $C_{82}H_{77}N_5O_5$: 1212.5; found: 1212.2 $[M]^+$, 1234.3 $[M + Na]^+$, 1250.2 $[M + K]^+$.

Tris-pyrene-(bromobenzyloxy)knotane 12: (*p*-Bromobenzyloxy)-knotane **6** (134 mg, 0.041 mmol), 4,4,5,5-tetramethyl-2-(1-pyrenyl)-1,3,2-dioxaborolane (**10**, 53.74 mg, 0.164 mmol) and 2′-dicyclohexylphosphanyl-2′,6′-dimethoxybiphenyl (**L***, 0.86 mg, 0.0021 mmol) were dissolved in toluene (24 mL). A solution of sodium carbonate (34.77 mg, 0.33 mmol) in water (6 mL) was added, after which the resulting mixture was flushed with argon for 15 min. After the addition of tetrakis(triphenyl)phosphanepalladium(0) (2.43 mg, 0.0021 mmol), the mixture was stirred in the dark at 115 °C under argon for 48 h. The reaction mixture was allowed to cool to room temp. and poured into a MeOH/water mixture. The precipitate was filtered off and, after leaching with dichloromethane, the solvent was removed under reduced pressure, yielding a mixture of the starting material and the tris-pyrene-substituted knotane. MALDI-TOF: *m*/*z*: calcd. for $C_{246}H_{228}N_{15}O_{15}$: 3637.65; found: 3638.0 $[M]^+$, 3660.0 $[M + Na]^+$, 3685.6 $[M + K]^+$.

Styrene-Substituted Knotanes 7a–c: Grubbs catalyst (dichlorobis-(tricyclohexylphosphyl)rutheniumbenzylidene, 8 mg, 0.01 mmol) was added under argon to a stirred solution of octenyloxy-knotane **6** (150 mg, 0.048 mmol) and styrene (31 mL, 0.30 mmol) in dry dichloromethane (25 mL). The reaction mixture was stirred under reflux for 24 h and the solvent was removed under reduced pressure, yielding a mixture of singly, doubly and triply styrene-substituted knotanes **7a**–**c**. MALDI-TOF: *m*/*z*: calcd. for $C_{207}H_{235}N_{15}O_{15}$ (**7a**): 3173.2; found: 3173.7 $[M]^+$; for $C_{213}H_{239}N_{15}O_{15}$ (**7b**): 3249.3; found: 3249.2 $[M]^+$; for $C_{219}H_{243}N_{15}O_{15}$ (**7c**): 3325.4; found: 3325.0 $[M]^+$; 3346.9 $[M + Na]^+$, 3362.7 $[M + K]^+$.

Triply Bridged Double Knot 8: Grubbs catalyst (dichlorobis(tricyclo-hexylphosphyl)rutheniumbenzylidene, 5 mg, 0.006 mmol) was added under argon to a stirred solution of octenyloxy-knotane **6** (100 mg, 0.032 mmol) in dry dichloromethane (250 mL). After the reaction mixture had been stirred under reflux for 24 h, the solvent was removed under reduced pressure. MALDI-TOF: *m*/*z*: calcd. for $C_{396}H_{450}N_{30}O_{30}$: 6110.0; found: 6112.0 $[M]^+$, 6131.7 $[M + Na]^+$, 6147.1 $[M + K]^+$.

Acknowledgments

The authors would like to thank the Deutsche Forschungsgemeinschaft (SFB 624) and the Alexander von Humboldt Foundation (F. W. V.) for financial support.

[1] a) G. Schill, *Catenanes, Rotaxanes and Knots*, Academic Press, New York, **1971**; b) N. C. Seeman, *J. Am. Chem. Soc.* **1992**, *114*, 9652–9655; c) S. M. Du, B. D. Stollar, N. C. Seeman, *J. Am. Chem. Soc.* **1995**, *117*, 1194–1200.

[2] a) *Molecular Catenanes, Rotaxanes and Knots, A Journey Through the World of Molecular Topology* (Eds.: J.-P. Sauvage, C. Dietrich-Buchecker), Wiley-VCH, Weinheim, **1999**; b) J.-P. Sauvage, C. Dietrich-Buchecker, *Molecular Knots – From Early Attempts to High-Yield Template Synthesis in Molecular Catenanes, Rotaxanes and Knots, A Journey Through the World of Molecular Topology* (Eds.: J.-P. Sauvage, C. Dietrich-Buchecker), Wiley-VCH, Weinheim, **1999**, pp. 107–142; c) L.-E. Perret-Aebi, A. von Zelewsky, C. Dietrich-Buchecker, J.-P. Sauvage, *Angew. Chem.* **2004**, *116*, 4582–4585.

[3] a) D. B. Amabilino, J. F. Stoddart, *Chem. Rev.* **1995**, *95*, 2725–2828; b) G. A. Breault, C. A. Hunter, P. C. Mayers, *Tetrahedron* **1999**, *55*, 5265–5293.

[4] O. Safarowsky, M. Nieger, R. Fröhlich, F. Vögtle, *Angew. Chem.* **2000**, *112*, 1699–1701; *Angew. Chem. Int. Ed.* **2000**, *39*, 1616–1618.

[5] F. Vögtle, A. Hünten, E. Vogel, S. Buschbeck, O. Safarowsky, J. Recker, A. Parham, M. Knott, W. M. Müller, U. Müller, Y. Okamoto, T. Kubota, W. Lindner, E. Francotte, S. Grimme, *Angew. Chem.* **2001**, *113*, 2534–2537; *Angew. Chem. Int. Ed.* **2001**, *40*, 2468–2471.

[6] a) O. Lukin, J. Recker, A. Böhmer, W. M. Müller, T. Kubota, Y. Okamoto, M. Nieger, F. Vögtle, *Angew. Chem.* **2003**, *115*, 458–461; *Angew. Chem. Int. Ed.* **2003**, *42*, 442–445; b) O. Lukin, W. M. Müller, U. Müller, A. Kaufmann, C. Schmidt, J. Leszczynski, F. Vögtle, *Chem. Eur. J.* **2003**, *9*, 3507–3517.

[7] Overview: O. Lukin, F. Vögtle, *Angew. Chem.* **2005**, *117*, 2–23; *Angew. Chem. Int. Ed.* **2005**, *44*, 2–23.

[8] N. Enomoto, S. Furukawa, Y. Ogasawara, H. Akano, Y. Kawamura, E. Yashima, Y. Okamoto, *Anal. Chem.* **1996**, *68*, 2798–2804.

[9] a) Y. Okamoto, M. Kawashima, K. Hatada, *J. Am. Chem. Soc.* **1984**, *106*, 5357–5359; b) Y. Okamoto, M. Kawashima, K. Hatada, *J. Chromatogr.* **1986**, *363*, 173–186.

[10] T. Zhang, D. Nguyen, P. Franco, T. Murakami, A. Ohnishi, H. Kurosawa, *Anal. Chim. Acta* **2006**, *557*, 221–228.

[11] The separation of **5a** was also successful on a Chiralpak®IB column with *n*-hexane/dichloromethane/ethanol (80:12:8) as eluent and a flow rate of 0.8 mL min^{-1}.

[12] a) H. Kuhn, D. Möbius, H. Bücher, *Physical Methods of Chemistry* (Eds.: A. Weisberger, B. Rossiter), vol. 1, part 3B, Wiley, New York, **1972**; b) H. Möhwald, *Thin Solid Films* **1988**, *159*, 1–15; c) G. L. Gaines, *Insoluble Monolayers at Liquid–Gas Interfaces*, Interscience, New York, **1966**.

[13] a) A. K. Chatterjee, T.-L. Choi, D. P. Sanders, R. H. Grubbs, *J. Am. Chem. Soc.* **2003**, *125*, 11360–11370; b) R. H. Grubbs (Ed.), *Handbook of Metathesis*, 3 volumes, Wiley-VCH, Weinheim, **2003**; c) R. H. Grubbs, *Tetrahedron* **2004**, *60*, 7117–7140.

[14] a) S. D. Walker, T. E. Barder, J. R. Martinelli, S. L. Buchwald, *Angew. Chem.* **2004**, *116*, 1907–1912; b) M. Masahiro, *Angew. Chem.* **2004**, *116*, 2251–2253.

Received: May 19, 2006
Published Online: September 4, 2006

